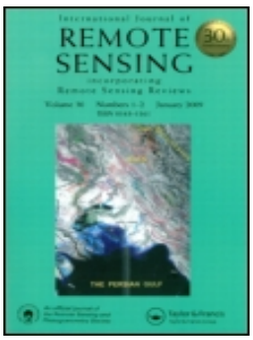

International Journal of Remote Sensing

ISSN: 0143-1161 (Print) 1366-5901 (Online) Journal homepage: http://www.tandfonline.com/loi/tres20

Assessment of forest damage caused by an ice storm using multi-temporal remote-sensing images: a case study from Guangdong Province

Jiansheng Wu, Tong Wang, Kuangyi Pan, Weifeng Li & Xiulan Huang

To cite this article: Jiansheng Wu, Tong Wang, Kuangyi Pan, Weifeng Li & Xiulan Huang (2016) Assessment of forest damage caused by an ice storm using multi-temporal remote-sensing images: a case study from Guangdong Province, International Journal of Remote Sensing, 37:13, 3125-3142, DOI: 10.1080/01431161.2016.1194544

To link to this article: http://dx.doi.org/10.1080/01431161.2016.1194544

INTERNATIONAL JOURNAL OF REMOTE SENSING, 2016
VOL. 37, NO. 13, 3125–3142
http://dx.doi.org/10.1080/01431161.2016.1194544

Taylor & Francis
Taylor & Francis Group

Assessment of forest damage caused by an ice storm using multi-temporal remote-sensing images: a case study from Guangdong Province

Jiansheng Wu[a,b], Tong Wang[a], Kuangyi Pan[c], Weifeng Li [d] and Xiulan Huang[a]

[a]Key Laboratory for Urban Habitat Environmental Science and Technology, Shenzhen Graduate School, Peking University, Shenzhen, P. R. China; [b]Key Laboratory for Earth Surface Processes, Ministry of Education, College of Urban and Environmental Sciences, Peking University, Beijing, P. R. China; [c]Department of Planning and Design, The Institution of Geological Surveying and Mapping, Zhejiang Province, Hangzhou, China; [d]Department of Urban Planning and Design, University of Hong Kong, Hong Kong, China

ABSTRACT

In early 2008, forest ecosystems in southern China suffered damage due to a severe ice storm disaster. The area and degree of forest damage caused by the ice storm was assessed using Satellite Pour l'Observation de la Terre (SPOT)-Vegetation images for Guangdong Province acquired between 1999 and 2008. By using the maximum value composition method and image thresholding techniques, the forest vegetation loss, expressed as the change in net primary productivity (NPP) and two indicators (I_1, I_2), was estimated. The damage threshold was determined by comparing the standard deviation of pixels of the undamaged areas in 2008 and other years without any disaster, which was 10%. The area of damaged forest vegetation was 47,670 km^2, with the northern Guangdong Province most seriously affected. The total loss of NPP for forest vegetation was 50,578,055 t (DW) year^{-1}, with 52 counties (43.7%) suffering forest vegetation damage. Evergreen coniferous forest was most widely affected, but evergreen broad-leaved forest was the most severely damaged vegetation type. Terrain topography influenced the damage to forest vegetation, which was found to increase with increasing elevation and slope gradient. The range and degree of damaged forest determined by remote-sensing data is consistent with the extent of the ice storm, indicating that this study provides a new approach for rapid assessment of forest disasters at a regional scale.

ARTICLE HISTORY
Received 29 May 2015
Accepted 23 May 2016

1. Introduction

Between 25 January and 6 February 2008, a rare period of extremely low temperatures and ice storms caused severe damage and loss of life in southern China. The direct economic loss was more than RMB 150 billion (10^9) (22 billion (10^9) USD) and 129 persons died. This disaster also caused severe damage to a number of forest areas (nearly 27.9 million (10^6) ha in southern China. It was estimated that the storm damaged

CONTACT Tong Wang wangtong@sz.pku.edu.cn Key Laboratory for Urban Habitat Environmental Science and Technology, Shenzhen Graduate School, Peking University, Room C-328, University Town, Nanshan District, Shenzhen 518055, P. R. China

11.9 million (10^6) ha of forest in Guangdong Province, which has a forest cover of 8.2% (Lin and Xue 2009), resulting in significant losses of forest ecosystem services.

Ice storms occur across large areas and usually cause extensive damage for a period time with accumulated ice and low temperature (Bragg, Shelton, and Zeide 2003). Ice storms are one of the most important non-biological disturbance factors for forest ecosystems in non-tropics (Millward, Kraft, and Warren 2010), and may cause serious damage to forest vegetation such as bending or uprooting of the tree trunks, as well as damage to the crowns.

Studies of forest damage have mainly concentrated on the damage to forest ecological services value and vegetation community structure caused by pests and disease (Olsson, Jönsson, and Eklundh 2012; Setiawan et al. 2014), fire (Arnett et al. 2015; Sedano et al. 2012), hurricane damage (Boose, Chamberlin, and Foster 2001; Kupfer et al. 2008; Ostertag, Silver, and Lugo 2005), and earthquakes (Jiang et al. 2015). Both ground survey and remote-sensing technology are common methods for forest damage evaluation. On the one hand, ground surveys can be employed to assess damage for a small area and focus on a specific type of vegetation community structure and plant physiology (Scarr, Hopkin, and Howse 2003). Remote-sensing approaches, on the other hand, enable fast assessment of large areas (Mildrexler et al. 2007; Näsi et al. 2015; Wang et al. 2010; Yi et al. 2013) and can efficiently monitor not only the extent of the damaged area but also the degree of this damage (Zhang et al. 2013). Multi-temporal imagery can detect the degree of damage and reduce to the minimum the errors caused by the fluctuation of vegetation indices and the influence of different growing period of different vegetation (Fransson et al. 2002; Verbesselt et al. 2010; Zhang et al. 2003).

Remote sensing has played an important role in ice storm damage research, because it can be used to compare the state of the forest vegetation explicitly before and after the storm (Olthof, King, and Lautenschlager 2004). For example, Isaacs et al. (2014) investigated ice storm damage across Ouachita National Forest in the United States using two sets of Landsat 7 ETM+ (Enhanced Thematic Mapper) images (before and after the storm) and demonstrated that not only topography but also biological and meteorological factors influence damage patterns in forests together. Environmental information, such as topography, may be effectively combined with ice storm patterns using satellite images. It has been found that topographic factors have a significant influence on the degree of forest damage (Stueve, Lafon, and Isaacs 2007). Additionally, different types of vegetation have different responses to damage (Lafon 2006; Millward and Kraft 2004; Smolnik, Hessl, and Colbert 2006).

Using Satellite Pour l'Observation de la Terre (SPOT)-Vegetation time-series data from 1999 to 2008 for Guangdong Province and image thresholding techniques, this study detected the forest damage threshold by analysing the changes in normalized difference vegetation index (NDVI) over the same period of every year. The goal of the research was to detect the scope and degree of forest damage caused by the 2008 ice storm, and to provide an approach to quickly evaluate forest damage over extensive areas with medium- and low-resolution satellite data.

2. Study area

Guangdong Province is located in southern China, at 20 ° 13 '–25° 31' N and 109° 39'–117° 19' E. The province is bordered by the Nanling Mountains to the north, the Wuyi

Mountains to the northeast, and by the South China Sea to the south. Guangdong Province covers a total area of 179,800 km^2, occupying 1.87% of China's land area. A variety of vegetation types are found within the province. Northern Guangdong is dominated by subtropical evergreen broad-leaved forest, which transitions into a subtropical monsoon forest in the central part of the province, and then to a tropical monsoon forest on the southern Leizhou Peninsula.

3. Data and methods

3.1. *Data acquisition*

For this study NDVI data, land-cover information, and digital elevation model (DEM) data were used. The NDVI data consisted of the product of SPOT-Vegetation, which is a synthesis of data strips from 10 consecutive days produced using the maximum value composition method, and was provided by the Flemish Institute for Technological Research (VITO), for the period beginning in April 1998. The data comprised a total of 360 images with a spatial resolution of 1 km, and covering the period from 1999 to 2008. Compared to other remote-sensing data, the advantage of SPOT-Vegetation data is that it has a high temporal resolution of 10 days, a spatial resolution of 1 km, which is appropriate for a province area (Cong et al. 2012), and an ability to better reflect seasonal vegetation changes.

For land-cover information, we selected the Global Land Cover 2000 (GLC-2000) data set provided by the European Union Joint Research Centre, with a spatial resolution of 1 km, including a total of nine land-cover types in Guangdong Province (Figure 1). The GLC-2000 projects were developed based on SPOT-4, which resulted in a good agreement between the NDVI and the land-cover data sets used in this study.

Shuttle Radar Topography Mission (SRTM) data provided by the United States National Aeronautics and Space Administration (NASA) and the United States Department of Defense's National Imagery and Mapping Agency (NIMA) were used as DEM data. Data resolution was 90 m and the data covered a total of four views of Guangdong Province.

3.2. *Data pre-processing*

All SPOT-Vegetation NDVI data for 1999–2008 were processed using the VGTExtract software for batch extraction and projection to the reference system WGS-84. The source data had already been corrected for atmospheric, radiometric, and geometric distortions, so it only needed to be transformed from digital number (DN) to NDVI values of the original images according to Equation (1) (Vegetation Program 1998):

$$\mathrm{NDVI} = 0.004d - 0.1, \tag{1}$$

where d is the digital number (DN) of image pixels.

In order to extract forest vegetation ranges from remote-sensing images for each year of the study period, evergreen broad-leaved forest, evergreen coniferous forest, and other natural forest types were selected from the land-cover maps as forest vegetation

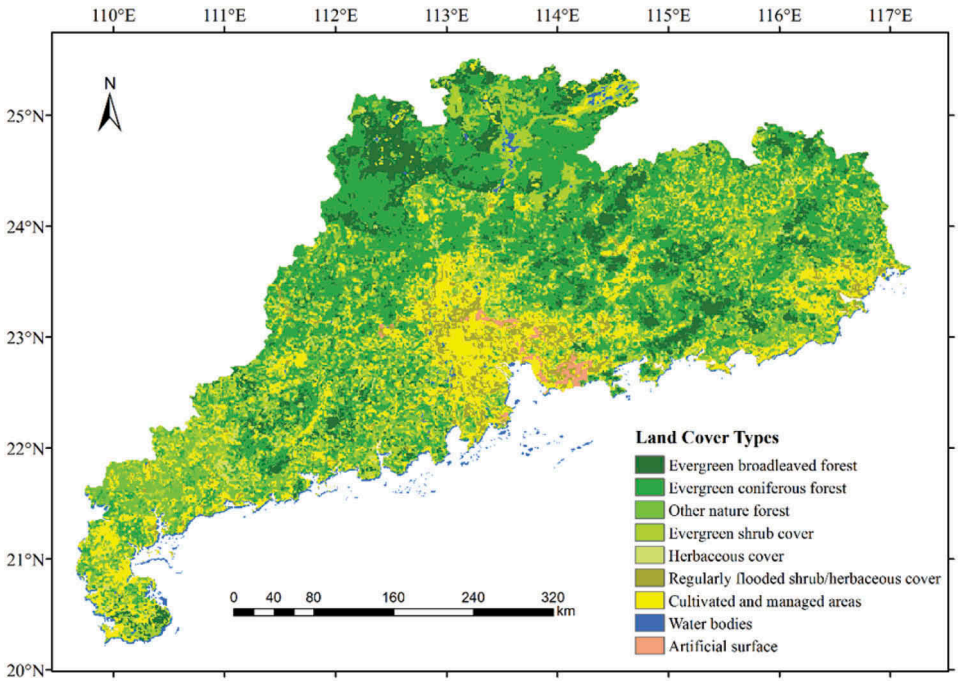

Figure 1. The land-cover types of Guangdong Province.

type objects. These three vegetation types represented the vegetation types that were most damaged by the 2008 ice storm. Damage to other vegetation types was not considered in this study.

3.3. *Time-series reconstruction of NDVI*

Ice and snow cover may lead to the decrease of real NDVI values, and it could not completely reflect damage degree by NDVI values before the leaves on the damaged trees wither. So, to reduce errors, we need to choose an appropriate study period in which snow melted and damaged vegetation completely died. Shaoguan and Qingyuan were the most severely damaged areas in this ice storm according to the ground survey data, so we extracted the NDVI curve of these areas to select the optimal time of the year for our research, with the goal of reducing errors to the minimum.

The NDVI data from 360 images were smoothed using TIMESAT software in order to reduce the interference of clouds, atmosphere, solar altitude angle, and sensor observations (Bradley et al. 2007). Because of its ability to correct abnormally low values (Chen et al. 2004), the Savitzky–Golay (SG) filter method (Savitzky and Golay 1964) was selected to smooth the data.

In order to reduce noise and improve data quality, the maximum NDVI (MNDVI) values for each year of the study period were calculated using the maximum value composition (MVC) method, resulting in a total of 10 images. The following equation was used:

$$m_i = \max_{j=1}^{n} (\mathrm{NDVI})_{i,j} \tag{2}$$

where m represents the MNDVI value, n is total number of images for each year of the study period, j represents the jth image in a year, i represents the ith image of the reconstructed data set.

3.4. *Image thresholding techniques*

Image thresholding techniques were applied to compare MNDVI values of the study period between the disaster year and other years. Spruce et al. (2011) used this method to evaluate pest damage of forest vegetation and identified a change rate of 4% as the damage threshold. They then detected the area with a variation greater than 4% as the pest damage region of the forest. The equation to calculate the NDVI variation is

$$V = \frac{m_{\mathrm{pre}} - m_{\mathrm{post}}}{m_{\mathrm{pre}}}\%, \tag{3}$$

where m_{pre} represents the average MNDVI value of the study period in other years, m_{post} is the MNDVI value for the same period in the disaster year, and V represents the variation rate of MNDVI value between the disaster year and other years during the same period.

Because the ice storm had caused serious damage to the forest ecosystem, a large number of branches and leaves covered the ground. This led to a reduction of forest biomass, which, in turn, led to a significant decrease of NDVI directly in the region of damaged forest and an increase of the NDVI standard deviation in an image (Wu, Chen, and Peng 2013). The standard deviation reflects the difference between the value of each pixel and the mean value of an image, and represents spatial variations of the NDVI image data. Standard deviation is normally used as an important parameter for segmentation of high-resolution images and multi-spectral image fusion, but is rarely used for threshold identification of multi-temporal images (Spruce et al. 2011). Based on the standard deviation of forest MNDVI images for each year of the study period, we varied the threshold from high to low according to variation rate of MNDVI in ArcGIS10.2, and compared the standard deviation of non-damaged areas (the region where value of V is greater than the threshold set) in 2008 to other years using the same threshold values. The forest damage threshold was determined as the value with a standard deviation for 2008 that was less than or equal to that of the other years, extrapolating the area beyond the scope of normal variation, which indicated the damage area caused by the ice storm.

3.5. *Forest damage assessment model*

To obtain a further quantitative evaluation of the ecological damage to the forest vegetation, we used net primary productivity (NPP) to measure the degree of vegetation damage in the damaged area. NPP was originally defined as the amount of photosynthetically fixed carbon available to the first heterotrophic level in an ecosystem (Field et al. 1998). Using the forest vegetation NPP model developed for China by Zheng and

Zhou (2000), which is based on the leaf area index (LAI) and NDVI, the degree of damage to the forest ecosystem can be calculated. The equation is written as follows:

$$\mathrm{NPP} = -0.6394 - 67.064 \ln(1 - (\mathrm{NDVI})). \tag{4}$$

Ground surveys of forest damage usually determine the degree of damage for prefectures, counties, or forest plantations with damaged forest area, but ignore the relative proportion of damaged areas within the forests, making it difficult to define different damage levels. At the prefecture level, this study defined two indices to evaluate the relative damage to a forest. These are the average damage of forest index (I_1) and the concentration of damage index (I_2). The equations for these two indices are as follows:

$$I_1 = (\mathrm{NPP})/f, \tag{5}$$

$$I_2 = (\mathrm{NPP})/d. \tag{6}$$

In these equations, f represents the forest area and d the damaged area. The I_1 index can be used to measure NPP loss per unit of forest area, while I_2 can evaluate the distribution of different degrees of forest damage.

4. Results and analysis

Based on the construction of SPOT-Vegetation NDVI time-series data sets, the period from mid-June to early July was chosen to be the study period. We used the image thresholding method to detect damage during 2008, and we found that the range and extent of damage assessed using time-series images data was in agreement with ground survey data.

Then loss amount of NPP values was calculated from NDVI, to quantify the degree of damage. Among the vegetation types, evergreen coniferous forest had the largest damage areas, but evergreen broad-leaved forest had the highest proportion of damage areas. Furthermore, terrain factors have a significant influence on forest damage.

4.1. *Time-series reconstruction of NDVI*

A 10-year average NDVI curve for forest vegetation within the severely damaged areas (Qingyuan and Shaoguan) was extracted and the S-G filter was applied for noise reduction (Figure 2(a)). After repeated testing and adjusting, the appropriate number of iterations was determined to be one, the envelope of fitting strength was two, and the S-G filter window was four. According to the NDVI curve for 2008 (Figure 2(b)), it is clear that NDVI values increased rapidly after the snow and ice began to melt in early February. Then, as damaged trees died and the normal variation of vegetation growth became dominant, NDVI decreased gradually until it started to pick up again in mid-April. This shows that the effects of damaged vegetation had been reduced to a minimum in mid-April, and NDVI values were more approximate to the undamaged vegetation. To minimize the impact of damaged trees that had not withered entirely and the effects of post-disaster restoration, the observation period should be set to the

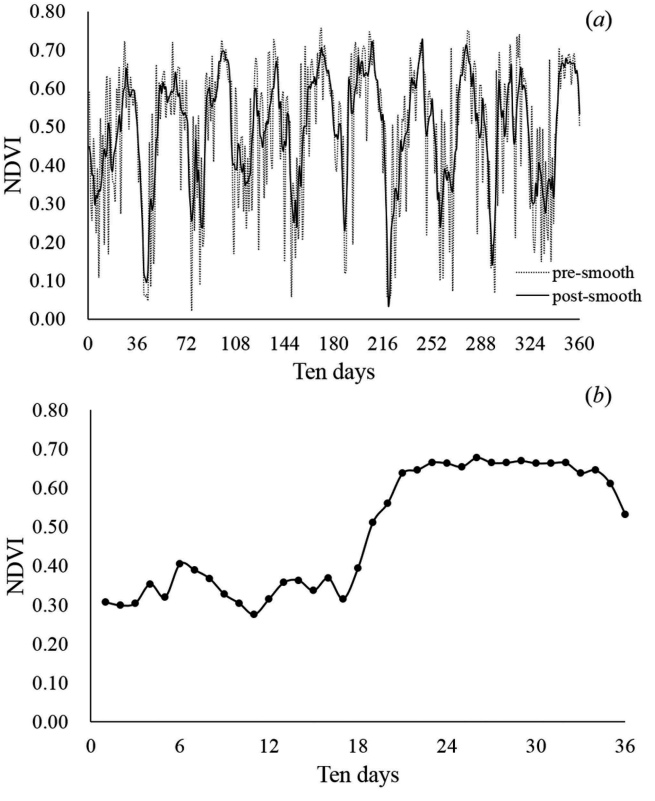

Figure 2. The S-G filtering results for NDVI in the serious disaster area (*a*) 1999–2008 (*b*) 2008.

vegetation-growing season after mid-April. Based on NDVI data quality, the period from mid-June to early July was finally chosen.

4.2. *Forest damage threshold*

Taking into account the quality of remote-sensing image data and the effects of other disasters (such as fires and hurricanes), we calculated the average and standard deviation for forest MNDVI images for the period of mid-June to early July from 1999 to 2008 (Figure 3), to select the years with higher data quality. It is obvious that the average for 2008 was lower and the standard deviation was higher due to the effect of the ice storm. Accordingly, we selected years in which the average was high and the standard deviation was low (the years 2000, 2001, 2003, 2004, 2006, and 2007), then used the average MNDVI during the study period as the normal level before the disaster, and calculated the variation of NDVI between 2008 and the other years according to Equation (3) for each grid. The variation values in some grids (Figure 4(a)) were less than zero; these grids represented the areas where MNDVI values for study period in 2008 were above the values of previous years. We removed these grids and normalized the remaining range of variation values to [0, 1] to arrive at the final variation rate distribution for MNDVI (Figure 4(b)).

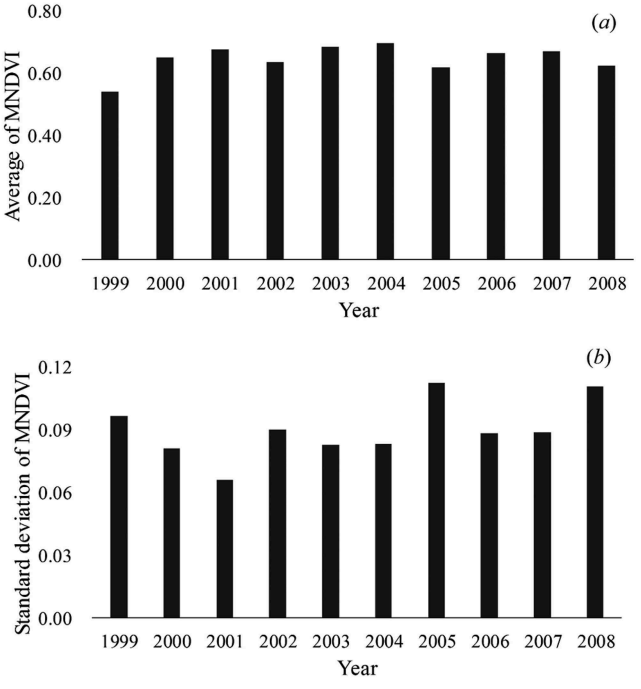

Figure 3. Average (*a*) and standard deviation (*b*) for MNDVI during the study period from 1999 to 2008.

Based on the change rate of MNDVI, we calculated the standard deviation of the unaffected area (where the change rate was lower than a certain threshold value) for 2008 and compared it to other years with the same threshold (Figure 5). Extrapolated from the maximum threshold, the standard deviation for the other years had remained relatively constant between 0.05 and 0.06, but the standard deviation for 2008 decreased gradually with decreasing threshold, forming a line of intersection at a threshold of 10%. Thus, the standard deviation for undamaged areas in 2008 was more similar to the same period in other years when removing the effects of disaster damage. So we analysed with a reverse order from 100% to 0%, and selected the threshold value when the standard deviation for 2008 was less than it was for other years. For example, we first calculated the standard deviation of NDVI for undamaged area in 2008 and other years with the threshold (the change rate of NDVI between 2008 and the other years) of 100%. If the standard deviation for 2008 was less than other years, 100% would be the damage threshold. Otherwise, we needed to calculate the next value of 99% in the same way. Finally we determined that the areas with MNDVI change rates of more than 10% were the areas of damaged forest vegetation.

4.3. *Scope and grades of forest damage*

Using a histogram of pixels above the damage threshold for 2008 (Figure 6), we divided the threshold into three levels based on the slope of the frequency distribution, and defined areas with a threshold above 40% as severe, between 24% and 40% as

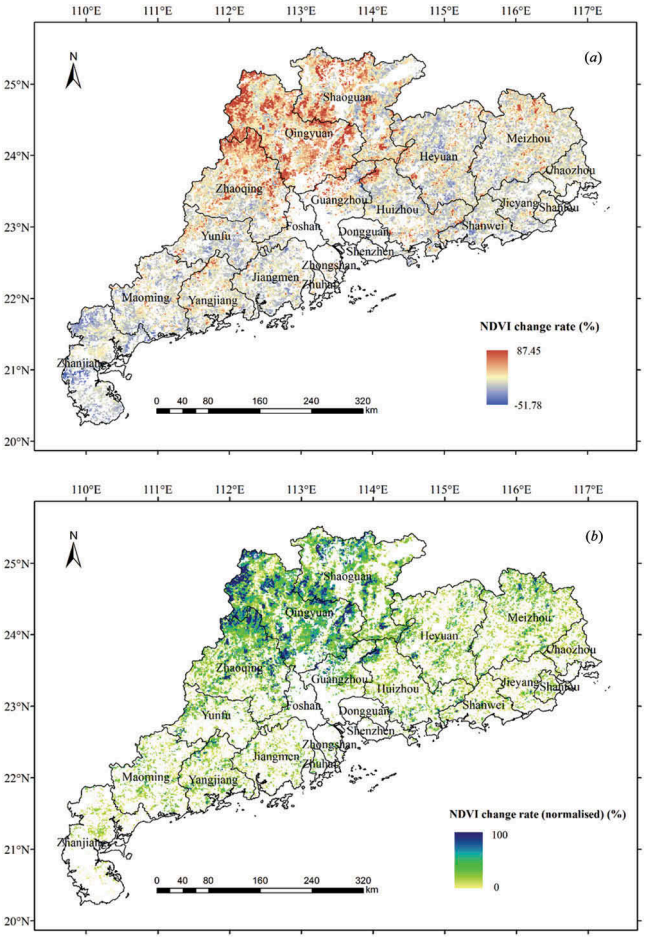

Figure 4. NDVI change rate between 2008 and other years (*a*) Unnormalized (*b*) Removed the grids with values less than 0 and normalised to [0,1].

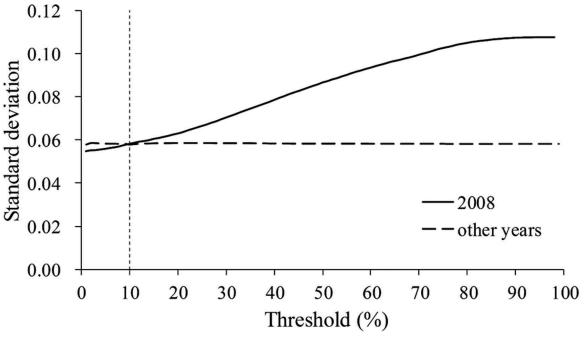

Figure 5. The relationship between threshold value and MNDVI standard deviation for unaffected areas.

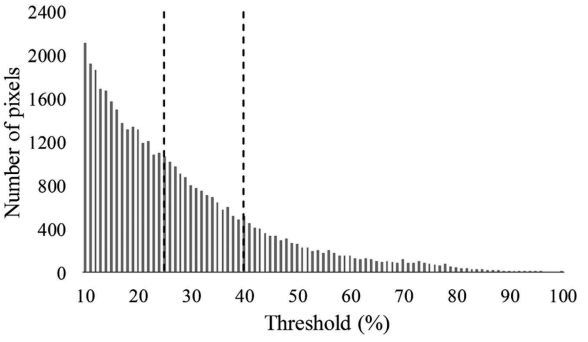

Figure 6. Histogram of the damage threshold.

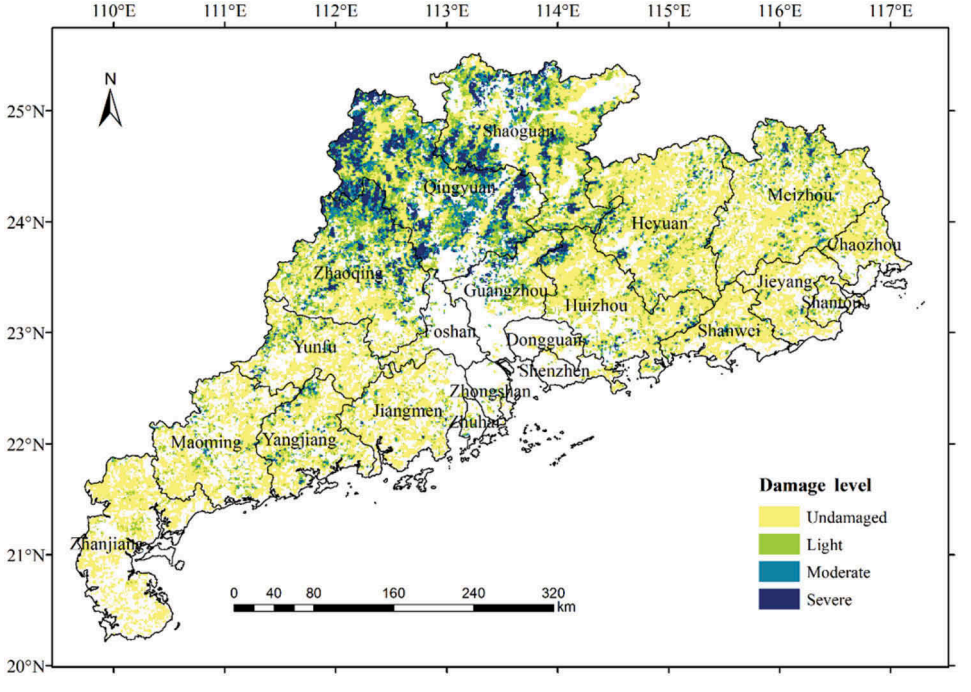

Figure 7. Distribution of forest damage levels in Guangdong.

moderate, between 10% and 24% as light, and the remaining areas as undamaged (Figure 7). There was a damaged area of 47,670 km^2 for the entire province, mainly concentrated in the northern part of Guangdong Province, including Zhaoqing, Qingyuan, Shaoguan, Heyuan, Meizhou, and Guangzhou, of which Qingyuan was the most seriously affected with 72% of the forest area damaged. Severe and moderate damage areas, which respectively accounted for 18.98% and 30.06% of damaged areas, were mainly located in Zhaoqing, Qingyuan, and Shaoguan. Areas with light damage were widespread, but were mainly found in the northern part of the province.

To investigate the accuracy of our results, we collected the ground survey data about the ice storm damage in 2008 (Lin and Xue 2009). According to this statistical

information, Guangdong Province had 7646.19 km^2 of severely damaged forest areas within provincial forest plantations, nature reserves, and Shaoguan, Qingyuan, Heyuan, Meizhou, Zhaoqing, occupying 8.2% of the total forest area in the province. Forest damage areas, based on remote-sensing images, were mainly located in northern Guangdong, which was consistent with the ground survey data. However, because of the different scales of remote-sensing images and damage survey statistics, as well as the accuracy of the damage level classification, the severely damaged area based on remote-sensing data in the province was 9046 km^2 and occupied 6.64% of the total forest area, which was slightly lower than the 8.2% mentioned above.

4.4. *Degree of forest damage*

After identifying the degree of forest damage by image thresholding techniques, NPP was used to measure the loss of forest ecosystems within the administrative region. Taking one pixel as the minimum research unit and considering the amount of MNDVI variation in 2008 compared to the other years, we estimated the loss of NPP using Equation (4) for the damaged areas (Figure 8). The unit for NPP is t (DW) hm^{-2} year^{-1}.

The NPP loss of forest vegetation in the province was 50,578,055 t (DW) year^{-1}, with the region of higher losses concentrated in the north-central part of the province. Taking counties as the analyses unit, this study considered the 48 counties where total losses of NPP were below 250,000 t (DW) year^{-1} as the undamaged region, which was almost completely located in the southern part of Guangdong Province. Of all 119 counties, 52 (43.7%) suffered disaster damage. Among them, the counties with relatively

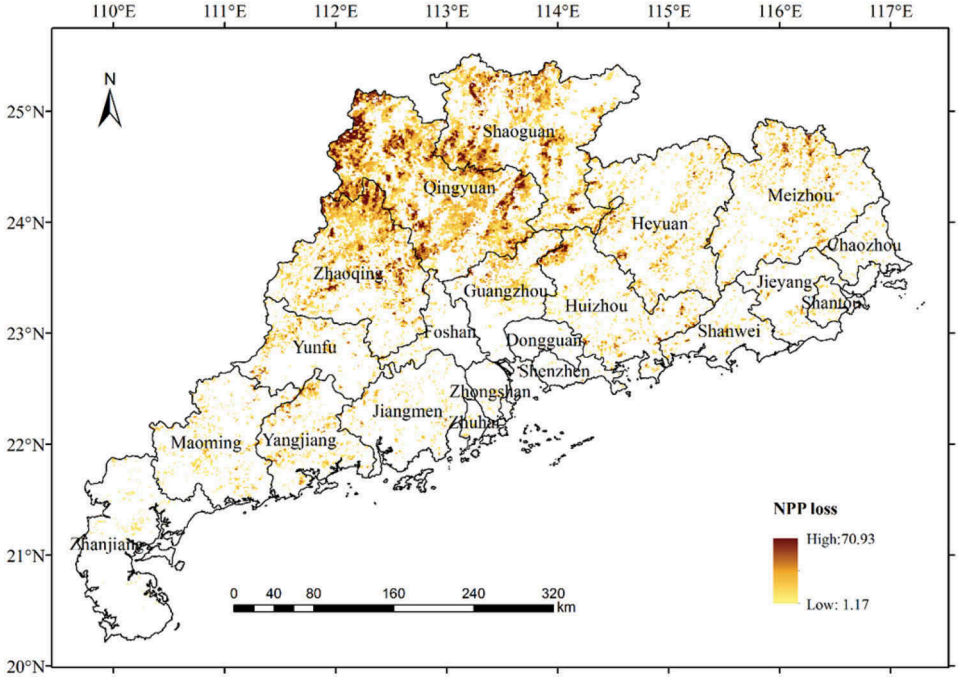

Figure 8. Distribution of NPP loss during the ice storm in Guangdong.

Table 1. Loss statistics for different prefectures.

Prefecture	Damage area (km^2)	Proportion of damage area (%)	Proportion of severely damage (%)	NPP loss (t (DW) $year^{-1}$)	I_1	I_2
Qingyuan	11,923	71.76	28.26	17,976,789	9.40	15.07
Shaoguan	7,709	54.03	22.08	10,249,290	6.23	13.29
Zhaoqing	6,373	52.32	20.34	8,273,414	5.91	12.98
Meizhou	3,083	24.72	8.47	2,943,483	2.05	9.54
Heyuan	2,873	22.66	8.46	2,656,816	1.82	9.24
Huizhou	2,076	24.84	15.46	2,149,649	2.24	10.35
Guangzhou	1,358	44.09	17.89	1,412,326	3.96	10.40
Yangjiang	1,253	24.88	9.34	1,183,696	2.05	9.44
Maoming	1,148	17.10	6.01	890,731	1.14	7.75
Yunfu	1,062	20.23	9.79	998,953	1.65	9.40
Jiangmen	680	13.68	4.71	498,537	0.86	7.33
Shanwei	381	11.74	8.14	308,785	0.83	8.10
Jieyang	301	9.66	5.65	236,306	0.65	7.85
Zhanjiang	274	4.70	0	134,448	0.19	4.90
Foshan	255	32.48	10.20	221,461	2.51	8.68
Chaozhou	219	11.24	2.28	147,871	0.65	6.75
Shantou	183	27.03	0	103,617	1.34	5.66
Zhongshan	97	40.59	12.37	77,662	2.84	8.01
Zhuhai	85	40.09	1.18	56,561	2.27	6.65
Dongguan	42	13.13	7.14	27,853	0.74	6.63
Shenzhen	41	11.36	7.32	29,807	0.69	7.27

I_1: Average Damage of Forest Index, I_2: Concentration of Damage Index.

concentrated disaster reports (including Lianzhou, Qujiang, Yangshan, Lchang, and Yingde) had a much higher loss of forest area and NPP than others; all of them were located in Shaoguan and Qingyuan prefectures.

Taking prefectures as the analysis unit, the statistics for disaster damage (Table 1) show that the indicators in Shaoguan, Zhaoqing, and Qingyuan are greater than in all other prefectures. In the remaining prefectures, I_1 shows a higher correlation with the proportion of damaged area of the prefecture, and prefectures that have a higher I_1 value, such as Meizhou, Guangzhou, Foshan, and others, also show a relatively higher proportion of damaged area. However, the prefectures listed as most severely affected in disaster survey statistics, such as Heyuan, have relatively low I_1 values, because the index is a measure for the proportion of NPP loss relative to the total forest area, regardless of the total affected area. On the other hand, severely damaged regions in the disaster survey statistics are usually regions with a large and concentrated damage area, while the I_1 index shows the actual percentage of damaged forest in each prefecture. Another indicator that I_2 can give a description of the concentration of damaged forest in the prefecture, and it shows a high correlation with the proportion of severely damaged area. The greater the index value is, the relatively more concentrated the severe damage area is, and the proportion of severe damage is also higher.

4.5. *Difference among forest vegetation types*

Table 2 shows the statistics of vegetation damaged according to the classification for different vegetation types. As evergreen coniferous forest covered the largest area in the province, the area of damage and loss of NPP was also highest. The proportion of severely damaged areas reached 20.87%, which was the highest percentage of the three kinds of vegetation that occur in the study area. Evergreen broad-leaved forest covered

Table 2. Loss statistics for different forest vegetation types.

Vegetation type	Area (km^2)	Damage area (km^2)	Proportion of damage area (%)	Proportion of severe damage (%)	NPP loss (t (DW) $year^{-1}$)	Proportion of NPP loss (%)
Evergreen broadleaved forest	23,978	8,581	35.79	18.32	10,781,707	21.86
Evergreen coniferous forest	91,044	28,228	31.00	20.87	36,090,450	73.18
Other nature forest	21,180	3,262	15.40	7.36	2,444,995	4.96

a smaller area than evergreen coniferous forest, occupying 17.6% of the province's forest. However, evergreen broad-leaved forest coverage in the damaged region was higher than the provincial average, so the damage area percentage (35.79%) was the highest compared to the other two types of vegetation, and the area of severe damage occupied 18.32% of the total damage area.

4.6. *Influence of topographical factors*

There have been a number of studies discussing the influence of topographical factors on forest vegetation damage (Isaacs et al. 2014; Martin and Ogden 2006; Stueve, Lafon, and Isaacs 2007). Most researchers agree that damage becomes more severe as elevation increases, while aspect does not show a significant influence. The impact of slope on vegetation is more obvious, and damage usually becomes more extensive as slopes become steeper. Considering the three major forest vegetation types, we investigated the damage to each vegetation type for different elevations, slopes, and aspects (Figure 9).

It was found that the impact of elevation for the three vegetation types is similar and showed as a decrease of damaged vegetation pixels with increasing elevation. However, the number of damage pixels increased with increasing altitude when considering the proportion of damage pixels to the total number of vegetation pixels. At 70–130 m and 300–400 m of elevation, the number of damage pixels and total pixels of evergreen broad-leaved forest both reached a maximum value. The amount of vegetation pixels increased constantly and reached a maximum value at 180–300 m, whereas the number of damage pixels remained constant, which means that this vegetation type suffered less damage within this elevation interval and suffered the most severe damage at elevations between 300 and 630 m. The amount of evergreen coniferous forest vegetation began to decline above 190 m elevation, but the proportion of damaged vegetation increased, with pixels indicating severe damage mainly concentrated at elevations between 370 and 600 m. The amount of other natural forest decreased rapidly as elevation increased, and was mainly concentrated at elevations below 100 m, which is similar to the overall trend of vegetation distribution.

Slope impact on vegetation damage is similar to the impact of elevation. Overall, the quantity of damage pixels decreased with increasing slope, but the proportion of total pixels indicating vegetation increased. Evergreen broad-leaved forest was dominant on slopes with angles below 20°, and severe damage mostly occurred at slope angles of

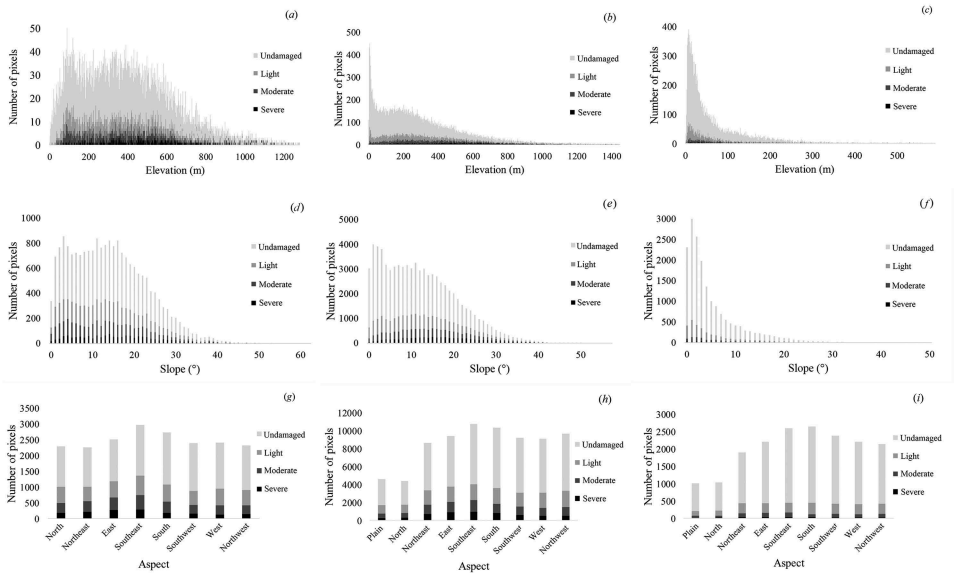

Figure 9. Statistic of damage pixels for different forest vegetation types in different topographies (*a*) Evergreen broad-leaved forest and elevation. (*b*) Evergreen coniferous forest and elevation. (*c*) Other nature forest and elevation. (*d*) Evergreen broad-leaved forest and slope. (*e*) Evergreen coniferous forest and slope. (*f*) Other nature forest and slope. (*g*) Evergreen broad-leaved forest and aspect. (*h*) Evergreen coniferous forest and aspect. (*i*) Other nature forest and aspect.

5–18°, while total damaged pixels reached a maximum in the 2–6° and 11–16° intervals. The amount of evergreen coniferous forest decreased gradually above 20°, which is similar to the distribution of evergreen broad-leaved forest, while severe damage and total damage mostly occurred in the 10–15° range. Other natural forest was less damaged, and mainly occurred on slopes with angles of 5° or less.

The influence of aspect is not same for the different vegetation types, and overall the number of damage pixels increases with the number of total vegetation pixels. East, southeast, south, and southwest aspects had the largest amount of vegetation but a relatively lower percentage of damage pixels, indicating that these aspects are conducive to the growth of vegetation.

Evergreen broad-leaved forest on the southeastern slopes had the largest amount and most severe damage, while the amount of severe damage was minimized on the western slopes. Distribution of damaged evergreen coniferous forests was similar to the total amount of vegetation, with the most serious damage being on the southeastern slopes. Other natural forest types had the most extensive damage on the southern and southeastern slopes, but the most serious damage on the northern and northeastern slopes.

5. Discussion and conclusions

Based on the construction of SPOT-Vegetation NDVI time-series data sets for 1999–2008 in Guangdong Province, we used a maximum value composition method to reconstruct MNDVI images for the period of mid-June to early July for each year. We compared the

MNDVI for each year calculated for the same period, and used an image thresholding method to detect the area and level of damage to forest vegetation during 2008. Then the loss amount of NPP values was calculated from NDVI, and two indices (I_1 and I_2) were used to assess damage to the forest caused by the 2008 ice storm. Finally, we compared the effects of different topographical factors on vegetation damage.

The range and extent of damage assessed using time-series images data is in agreement with ground survey data collected after the ice storm. This study compared the standard deviations for 2008 and other years without damage for undamaged areas using the same threshold conditions. We identified 10% as the damage threshold, resulting in an affected forest area of 47,670 km^2, in which severe damage accounted for 6.64% of the province's forest area. The most severe damage was mainly concentrated in northern Guangdong, while the southern coastal area was mostly undamaged. The NPP loss of forest vegetation caused by the ice storm in the province amounted to 50,578,055 t (DW) year^{-1}. Of all 119 counties, 52 (43.7%) suffered disaster damage, with Lianzhou, Qujiang, Yangshan, and Lechang being the most seriously affected counties. In prefectures, the building concentration of damage index and the average amount of forest damage index, showed the relative degree of damage for each prefecture. Our research showed that this approach is applicable for large areas to rapidly assess and simulate the spatial distribution of damage to forests.

The impact of topographical factors on different damaged forest vegetation types showed that the amount of damage pixels increased with increasing elevation and slope, and that the impact of aspect depended on specific circumstances. This is because the high elevation area and steeper slope area has much more snow cover, and snow melts more slowly than lower elevation area and lower slope area (Li et al. 2005). Furthermore, the steeper the slope, the more trees there are with asymmetric canopy (Nykänen et al. 1997). In general, the southern aspect receives much more sunshine, which makes snow melt faster, so the vegetation on these aspects suffers less damage in an ice storm.

For this particular disaster in 2008, evergreen coniferous forest had the largest damage areas, but evergreen broad-leaved forest had the highest proportion of damage areas. The reason may be that the trees in evergreen broad-leaved forest have a larger leaf area, so they will carry more snow on the leaf surface.

Although using remote-sensing images can quickly assess the scope and extent of forest damage, it is recommended to combine remote sensing with field surveys to reduce errors for some areas. The GLC-2000 land-cover data used in this study matched the SPOT-Vegetation data well because they were both based on SPOT-4 satellite data, but these data were recorded in 2000, and large areas of forest may have changed in the following years, which may have influence on the final results. In addition, the NPP estimation model based on NDVI is too simple, and was insufficient in dealing with complex conditions. We suggest that incorporating temperature and rainfall data with the NDVI time-series during ice storm disasters will produce better NPP estimates and will make estimates of forest damage more precise.

Acknowledgement

This work was supported by the State Key Program of National Natural Science of China 'Correlation between urban landscape pattern and ecological risk due to natural disasters: A case study in Shenzhen City' (NO.41330747).

Disclosure statement

No potential conflict of interest was reported by the authors.

Funding

This work was supported by the State Key Program of National Natural Science of China 'Correlation between urban landscape pattern and ecological risk due to natural disasters: A case study in Shenzhen City' [grant number 41330747].

ORCID

Weifeng Li http://orcid.org/0000-0001-5386-3019

References

Arnett, J. T. T. R., N. C. Coops, L. D. Daniels, and R. W. Falls. 2015. "Detecting Forest Damage after a Low-Severity Fire Using Remote Sensing at Multiple Scales." *International Journal of Applied Earth Observation and Geoinformation* 35: 239–246. doi:10.1016/j.jag.2014.09.013.

Boose, E. R., K. E. Chamberlin, and D. R. Foster. 2001. "Landscape and Regional Impacts of Hurricanes in New England." *Ecological Monographs* 71: 27–48. doi:10.1890/0012-9615(2001)071[0027:LARIOH]2.0.CO;2.

Bradley, B. A., R. W. Jacob, J. F. Hermance, and J. F. Mustard. 2007. "A Curve Fitting Procedure to Derive Inter-Annual Phenologies from Time Series of Noisy Satellite NDVI Data." *Remote Sensing of Environment* 106: 137–145. doi:10.1016/j.rse.2006.08.002.

Bragg, D. C., M. G. Shelton, and B. Zeide. 2003. "Impacts and Management Implications of Icestorms on Forests in the Southern United States." *Forest Ecology and Management* 186: 99–123. doi:10.1016/S0378-1127(03)00230-5.

Chen, J., P. Jönsson, M. Tamura, Z. Gu, B. Matsushita, and L. Eklundh. 2004. "A Simple Method for Reconstructing A High-Quality NDVI Time-Series Data Set Based on the Savitzky-Golay Filter." *Remote Sensing of Environment* 91: 332–344. doi:10.1016/j.rse.2004.03.014.

Cong, N., S. Piao, A. Chen, X. Wang, X. Lin, S. Chen, S. Han, G. Zhou, and X. Zhang. 2012. "Spring Vegetation Green-Up Date in China Inferred from SPOT NDVI Data: A Multiple Model Analysis." *Agricultural and Forest Meteorology* 165: 104–113. doi:10.1016/j.agrformet.2012.06.009.

Field, C. B., M. J. Behrenfeld, J. T. Randerson, P. Falkowsk. 1998. "Primary Production of the Biosphere: Integrating Terrestrial and Oceanic Components." *Science* 281: 237–240. doi:10.1126/science.281.5374.237.

Fransson, J. E. S., F. Walter, K. Blennow, A. Gustavsson, and L. M. H. Ulander. 2002. "Detection of Storm-Damaged Forested Areas Using Airborne CARABAS-II VHFSAR Image Data." *IEEE Transactions on Geoscience and Remote Sensing* 40: 2170–2175. doi:10.1109/TGRS.2002.804913.

Isaacs, R. E., K. M. Stueve, C. W. Lafon, and A. H. Taylor. 2014. "Ice Storms Generate Spatially Heterogeneous Damage Patterns at the Watershed Scale in Forested Landscapes." *Ecosphere* 5: 141. doi:10.1890/ES14-00234.1.

Jiang, W., K. Jia, J. Wu, Z. Tang, W. Wang, and X. Liu. 2015. "Evaluating the Vegetation Recovery in the Damage Area of Wenchuan Earthquake Using MODIS Data." *Remote Sensing* 7: 8757–8778. doi:10.3390/rs70708757.

Kupfer, J. A., A. T. Myers, S. E. McLane, and G. N. Melton. 2008. "Patterns of Forest Damage in a Southern Mississippi Landscape Caused by Hurricane Katrina." *Ecosystems* 11: 45–60. doi:10.1007/s10021-007-9106-z.

Lafon, C. W. 2006. "Forest Disturbance by Ice Storms in Quercus Forests of the Southern Appalachian Mountains, USA." *Ecoscience* 13: 30–43. doi:10.2980/1195-6860(2006)13[30:FDBISI]2.0.CO;2.

Li, X. F., J. J. Zhu, Q. L. Wang, and Z. G. Liu. 2005. "Forest Damage Induced by Wind/Snow: A Review." *Acta Ecological Sinica* 25: 148–157.

Lin, Y., and C. Xue. 2009. "The Planning and Technology of Post-Frost Forest Ecological Rehabilitation in Guangdong Province." *Guangdong Forestry Science and Technology* 25: 102–106.

Martin, T. J., and J. Ogden. 2006. "Wind Damage and Response in New Zealand Forests: A Review." *New Zealand Journal of Ecology* 30: 295–310.

Mildrexler, D. J., M. Zhao, F. A. Heinsch, and S. W. Running. 2007. "A New Satellite-Based Methodology for Continental-Scale Disturbance Detection." *Ecological Applications* 17: 235–250. doi:10.1890/1051-0761(2007)017[0235:ANSMFC]2.0.CO;2.

Millward, A. A., and C. E. Kraft. 2004. "Physical Influences of Landscape on a Large-Extent Ecological Disturbance: The Northeastern North American Ice Storm of 1998." *Landscape Ecology* 19: 99–111. doi:10.1023/B:LAND.0000018369.41798.2f.

Millward, A. A., C. E. Kraft, and D. R. Warren. 2010. "Ice Storm Damage Greater along the Terrestrial-Aquatic Interface in Forested Landscapes." *Ecosystems* 13: 249–260. doi:10.1007/s10021-010-9314-9.

Näsi, R., E. Honkavaara, P. Lyytikäinen-Saarenmaa, M. Blomqvist, P. Litkey, T. Hakala, N. Viljanen, T. Kantola, T. Tanhuanpää, and M. Holopainen. 2015. "Using UAV-Based Photogrammetry and Hyperspectral Imaging for Mapping Bark Beetle Damage at Tree-Level." *Remote Sensing* 7: 15467–15493. doi:10.3390/rs71115467.

Nykänen, M.-L., H. Peltola, C. Quine, S. Kellomäki, and M. Broadgate. 1997. "Factors Affecting Snow Damage of Trees with Particular Reference to European Conditions." *Silva Fennica* 31: 193–213. doi:10.14214/sf.a8519.

Olsson, P., A. M. Jönsson, and L. Eklundh. 2012. "A New Invasive Insect in Sweden – Physokermes Inopinatus: Tracing Forest Damage with Satellite Based Remote Sensing." *Forest Ecology and Management* 285: 29–37. doi:10.1016/j.foreco.2012.08.003.

Olthof, I., D. J. King, and R. A. Lautenschlager. 2004. "Mapping Deciduous Forest Ice Storm Damage Using Landsat and Environmental Data." *Remote Sensing of Environment* 89: 484–496. doi:10.1016/j.rse.2003.11.010.

Ostertag, R., W. L. Silver, and A. E. Lugo. 2005. "Factors Affecting Mortality and Resistance to Damage following Hurricanes in a Rehabilitated Subtropical Moist Forest." *Biotropica* 37: 16–24. doi:10.1111/btp.2005.37.issue-1.

Savitzky, A., and M. Golay. 1964. "Smoothing and Differentiation of Data by Simplified Least Squares Procedures." *Analytical Chemistry* 36: 1627–1639. doi:10.1021/ac60214a047.

Scarr, T. A., A. A. Hopkin, and G. M. Howse. 2003. "Aerial Sketch-Mapping of the 1998 Ice Storm in Eastern Ontario." *The Forestry Chronicle* 79: 91–98. doi:10.5558/tfc79091-1.

Sedano, F., P. Kempeneers, P. Strobl, D. McInerney, and J. San Miguel. 2012. "Increasing Spatial Detail of Burned Scar Maps Using IRS-AWiFS Data for Mediterranean Europe." *Remote Sensing* 4: 726–744. doi:10.3390/rs4030726.

Setiawan, N. N., M. Vanhellemont, L. Baeten, M. Dillen, and K. Verheyen. 2014. "The Effects of Local Neighbourhood Diversity on Pest and Disease Damage of Trees in a Young Experimental Forest." *Forest Ecology and Management* 334: 1–9. doi:10.1016/j.foreco.2014.08.032.

Smolnik, M., A. Hessl, and J. J. Colbert. 2006. "Species-Specific Effects of a 1994 Ice Storm on Radial Tree Growth in Delaware." *The Journal of the Torrey Botanical Society* 133: 577–584. doi:10.3159/1095-5674(2006)133[577:SEOAIS]2.0.CO;2.

Spruce, J. P., S. Sader, R. E. Ryan, J. Smoot, P. Kuper, K. D. Ross, D. Prados, J. Russell, G. Gasser, and R. McKellip. 2011. "Assessment of MODIS NDVI Time-Series Data Products for Detecting Forest Defoliation by Gypsy Moth Outbreaks." *Remote Sensing of Environment* 115: 427–437. doi:10.1016/j.rse.2010.09.013.

Stueve, K. M., C. W. Lafon, and R. E. Isaacs. 2007. "Spatial Patterns of Ice Storm Disturbance on a Forested Landscape in the Appalachian Mountains, Virginia." *Area* 39: 20–30. doi:10.1111/area.2007.39.issue-1.

Vegetation Program. 1998. SPOT Vegetation User Guide. http://www.spotimage.fr/data/images/vege/vegetat/book_1/e_frame.htm.

Verbesselt, J., R. Hyndman, A. Zeileis, and D. Culvenor. 2010. "Phenological Change Detection while Accounting for Abrupt and Gradual Trends in Satellite Image Time Series." *Remote Sensing of Environment* 114: 2970–2980. doi:10.1016/j.rse.2010.08.003.

Wang, W., J. J. Qu, X. Hao, Y. Liu, and J. A. Stanturf. 2010. "Post-Hurricane Forest Damage Assessment Using Satellite Remote Sensing." *Agricultural and Forest Meteorology* 150: 122–132. doi:10.1016/j.agrformet.2009.09.009.

Wu, J., S. Chen, and J. Peng. 2013. "Assessment of Forest Damage Due to Ice Storm Using Image Thresholding Techniques: A Case Study of Yunnan Province." *Progress in Geography* 32: 913–923.

Yi, K., H. Tani, J. Zhang, M. Guo, X. Wang, and G. Zhong. 2013. "Long-Term Satellite Detection of Post-Fire Vegetation Trends in Boreal Forests of China." *Remote Sensing* 5: 6938–6957. doi:10.3390/rs5126938.

Zhang, X., Y. Wang, H. Jiang, and X. Wang. 2013. "Remote-Sensing Assessment of Forest Damage by Typhoon Saomai and Its Related Factors at Landscape Scale." *International Journal of Remote Sensing* 34: 7874–7886. doi:10.1080/01431161.2013.827344.

Zhang, X. Y., M. A. Friedl, C. B. Schaaf, A. H. Strahler, J. Hodges, F. Gao, B. C. Reed, and A. Huete. 2003. "Monitoring Vegetation Phenology Using MODIS." *Remote Sensing of Environment* 84: 471–475. doi:10.1016/S0034-4257(02)00135-9.

Zheng, Y., and G. Zhou. 2000. "A Forest Vegetation NPP Model Based on NDVI." *Acta Phytoecologica Sinica* 24: 9–12.